NUMERICAL STUDY OF 3-D CONSTRAINT EFFECTS IN SE(B) SPECIMENS

Emerson G. Rabello
Julio R. B. Cruz
egr@cdtn.br
jrbc@cdtn.br
Centro de Desenvolvimento da Tecnologia Nuclear - CDTN/CNEN
Caixa Postal 941, CEP 30123-970, Belo Horizonte, MG, Brasil

Miguel M. Neto
Carlos A. J. Miranda
mmattar@ipen.br
cmiranda@ipen.br
Instituto de Pesquisas Energéticas e Nucleares - IPEN/CNEN
Caixa Postal 11049, CEP 05422-970, São Paulo, SP, Brasil

Abstract. *In standard fracture toughness testing, the specimens' configurations should comply with size requirements regarding the initial crack length and the thickness of the specimen. These restrictions are mainly to ensure a plane strain condition at the crack tip, and thus to obtain a plane strain toughness. However, to obtain relevant material toughness for assessing real structures with shallow cracks and/or small thickness, various types of non-standard testing specimens, with different thickness and crack lengths, should be tested. To properly interpret testing results of non-standard specimens, it is necessary to understand and take into account the in-plane and out-of-plane constraint effects from experimental data.*
Different approaches have been proposed to quantify constraint and to describe the effects of constraint variations on engineering fracture toughness characterized by J-integral, or equivalently the crack tip opening displacement, CTOD. This paper presents the results of a numerical investigation, in which single-edge cracked bars in three point bend SE(B) specimens, with different relative crack lengths and thickness, were systematically studied via detailed three-dimensional finite element analyses. A new parameter is then proposed to quantify crack tip constraint.

Keywords: *J-integral, Crack tip constraint, Q-Parameter, Finite-Elements Analysis (FEA).*

1. INTRODUCTION

One of the fundamental assumptions of fracture mechanics is that the crack tip conditions can be uniquely characterized by a single parameter such as the stress intensity factor K or the J-integral. When this assumption is valid, the critical value of the crack tip parameter represents a size independent measure of the fracture toughness. This situation occurs in small-scale yielding (SSY) conditions, when the size of the plastic zone remains small compared to the specimen external geometry. However, for large-scale yielding (LSY) in finite bodies, the relationship between the scaling parameter (i.e. J-integral), and the near-tip fields loses the one-to-one correspondence. This loss of uniqueness, often termed loss of constraint, produces the increases in fracture toughness observed for tension geometries and for shallow notch bend specimens.

In standard fracture toughness testing, the specimens' configurations should comply with size requirements regarding the initial crack length and the thickness of the specimen. These restrictions are mainly to ensure a plane strain condition at the crack tip, and thus to obtain a plane strain toughness. However, to obtain relevant material toughness for assessing real structures with shallow cracks and/or small thickness, various types of non-standard testing specimens, with different thickness and crack lengths, should be tested. To properly interpret testing results of non-standard specimens, it is necessary to understand and take into account the in-plane and out-of-plane constraint effects from experimental data.

Different approaches have been proposed to quantify constraint and to describe the effects of constraint variations on engineering fracture toughness characterized by J-integral, or equivalently the crack tip opening displacement, CTOD. The J-Q methodology developed by O'Dowd and Shih (1991, 1992) is one of the main theories used to describe the constraint effects in fracture toughness. In this methodology, the J-integral sets the size scale over which large deformations and high stresses develop while the additional parameter (Q) quantifies the level of stress triaxiality ahead of the crack tip. Under increased loading, each fracture specimen follows a characteristic driving force curve, or trajectory, which defines the evolution of crack-tip deformation (J) and constraint (Q).

This paper presents the results of a numerical investigation, in which single-edge cracked bars in three point bend SE(B) specimens, with different relative crack lengths and thickness, were systematically studied via detailed three-dimensional finite element analyses. A new parameter is then proposed to quantify crack tip constraint.

2. J-Q METHODOLOGY

The J-Q description of mode I, plane-strain crack tip fields derives initially from consideration of the boundary layer model for small-scale yielding (SSY). Crack-tip stresses for linear elastic conditions have the form show in Eq. (1) (Willians, 1957).

$$\sigma_{ij} = \frac{K_I}{\sqrt{2\pi r}} f_{ij}(\theta) + T\,\delta_{1i}\cdot\delta_{1j} \tag{1}$$

Here, r and θ are polar coordinates centered at the crack tip, with θ = 0 corresponding to the line ahead of the crack, and $K_I = \sqrt{EJ/(1-\upsilon^2)}$, where J denotes Rice's J-integral (Rice, 1986). E is the Young's modulus and ν is the Poisson's ratio. Crack tip fields differing in stress triaxiality are generated by varying the non-singular stress, T, parallel to the crack plane. In the computational model for SSY, the conditions defined by Eq. (1) are imposed

incrementally on the remote outer boundary of a symmetrically constrained, semi-circular mesh of elements focused on the crack tip.

O'Dowd and Shih (1991, 1992) employed asymptotic analyses and detailed finite element analyses to propose the approximate two-parameter description of the crack tip fields, which applies under small and large-scale yielding conditions:

$$\sigma_{ij} = \sigma_0 f_{ij}\left(\frac{r}{J/\sigma_0}, \theta, Q\right) \qquad \varepsilon_{ij} = \varepsilon_0 g_{ij}\left(\frac{r}{J/\sigma_0}, \theta, Q\right) \tag{2}$$

The dimensionless second parameter, Q, in Eq. (2) defines the amount by which σ_{ij} and ε_{ij} in fracture specimens differ from the adopted SSY reference solution at the same applied J.

To a good approximation, O'Dowd and Shih showed that $Q\sigma_0$ represents the difference in hydrostatic stress over the forward sector ahead of the crack tip between the SSY and fracture specimen fields. Thereby, operationally, Q is defined by:

$$Q \equiv \frac{\sigma_{\theta\theta} - (\sigma_{\theta\theta})_{SSY}}{\sigma_0}, \quad at\ \theta = 0, \quad r = 2J/\sigma_0 \tag{3}$$

where the specimen stresses ($\sigma_{\theta\theta}$) in Eq. (3) are evaluated from finite element analyses containing sufficient mesh refinement to resolve the fields at this length scale ($r = 2J/\sigma_0$).

At low deformation levels, fracture specimens experience SSY conditions and Q remains very nearly zero. Once large-scale yielding conditions prevail, hydrostatic stresses at the crack tip are substantially less than those in SSY at the same J-value. This difference produces negative Q values once the specimen deviates from SSY conditions. For deeply notched SE(B) and C(T) specimens, the elastic T-stress is positive and thus Q takes on slightly positive values at low deformation levels before constraint loss occurs.

3. COMPUTATIONAL ANALYSES

This paper presents the results of a numerical investigation, in which single-edge cracked bars in three point bend SE(B) specimens, with different relative crack lengths and thickness, were systematically studied via detailed non-linear three-dimensional finite element analyses.

The studied specimen is presented in Fig. 1, where crack length, width and thickness are denoted by a, W and B, respectively. To consider the specimen thickness effect, three values of B/W are considered: 0.5, 0.25 and 0.125. In terms of in-plane constraint, three different values of a/W are considered: 0.100, 0.250 and 0.500.

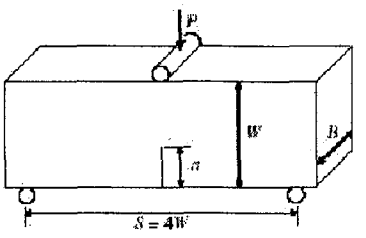

Figure 1- Single-edge cracked bar in three points bend SE(B) specimen.

Figure 2 depicts typical 3-D FE meshes employed in the present work. Finite element meshes typically have about 12,000 elements (8-node hexahedron elements). Symmetry

conditions, fully utilized for efficient computation, enabled the use of one-quarter models as indicated. Ten elements are used to resolve the stress gradient along the thickness direction.

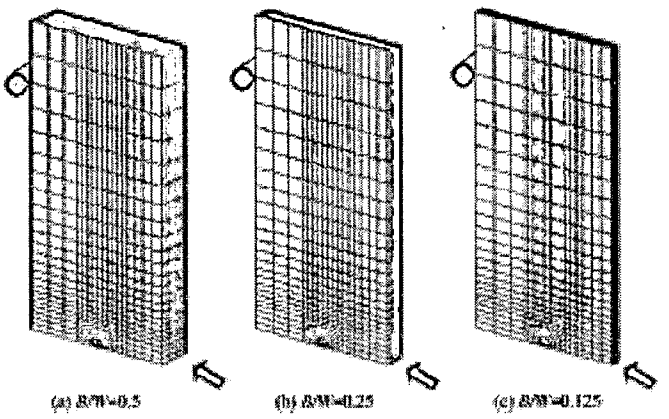

Figure 2- Typical 3-D FE meshes employed in the present work.

The uniaxial stress-strain curve follows a linear then power-law model given by Ramberg-Osgood equation.

$$\frac{\varepsilon}{\varepsilon_0}=\frac{\sigma}{\sigma_0} \quad \varepsilon \le \varepsilon_0; \quad \frac{\varepsilon}{\varepsilon_0}=\left(\frac{\sigma}{\sigma_0}\right)^n \quad \varepsilon > \varepsilon_0 \tag{4}$$

where ε_0 and σ_0 define limits for the initial linear portion of the response. All computations use $E/\sigma_0 = 500$ and Poisson's ratio $\nu = 0.3$. On the other hand, three values of n (5, 10 and 20), are considered, which are believed to cover practically interesting ranges for fracture toughness testing of typical materials.

Finite elements results were generated with the research code WARP3D (Koppenhoefer et al., 2002) which employs an incrementally iterative Newton procedure to resolve the nonlinear equilibrium equations.

The conventional 8-node hexahedron element exhibits severe volumetric locking under incompressible plastic deformation. The WARP3D code adopts the $\overline{B}$ modification suggested by Hughes (Hughes, 1980) to alleviate the locking behavior.

The local energy release rate for Mode I crack extension at each point along the front is given by:

$$J = \lim_{\Gamma \to 0} \int_{\Gamma} W\, n_1 - \sigma_{ij} \frac{\delta u_i}{\delta x_1} n_j \, d\Gamma \tag{5}$$

where W denotes the strain-energy density, Γ is a vanishingly small contour in the principal normal plane at n is a unit normal vector to Γ, σ_{ij} and u_i are Cartesian components of stress in the crack front coordinate system. In the present analyses, numerical evaluation of Eq. (5) is accomplished with a domain integral method (Shih et al., 1986) as implemented in WARP3D. The resulting formulation provides pointwise values of J across the crack front at each thickness layer and thickness average value at each loading level.

Q-Parameter was obtained along the thickness using the JQCRACK program (Cravero et al., 2003). The SSY reference fields required for Q computations are obtained from plane-strain, finite element solutions of the modified boundary layer model of an infinite body, single-ended crack problem (Al-Ani et al., 1991).

4. RESULTS AND DISCUSSION

The J-Integral and Q-Parameter values along the thickness (normalized by B_x/B_T, where B_T is the total thickness) are presented in Fig. 3. It was observed that the J-Integral values decrease strongly along the thickness. An inverse behavior occurred with the Q-Parameter. This effect becomes more pronounced for higher loads. All analyzed configurations presented a similar behavior.

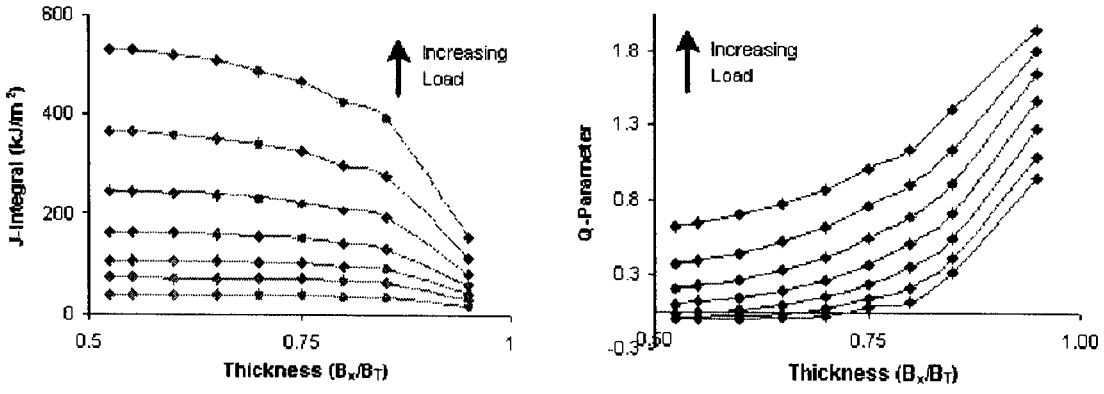

Figure 3- Integrals and Q-Parameter values along the thickness.
(Specimen SE(B), a/W = 0.500, B/W = 0.5 and n = 05)

The decrease of the J-Integral values and the increase of the Q-Parameter along the thickness reveal the in-plane and out-of-plane constraint effects in the specimens. Thereby, a new parameter (Q_{3D}) is proposed to characterize the constraint effects along the thickness:

$$Q_{3D} = 2 \cdot \int_{B_x=0.5}^{B_x=1} Q(B_x)\, dB_x \qquad (6)$$

where $Q(B_x)$ is the value of the Q-Parameter in each point of the thickness and the constant 2 is associated to the used symmetry.

The Q_{3D}-*Parameter* corresponds to the area under the curve Q-Parameter vs. Thickness and represents a combination of the in-plane and out-of-plane constraint effects in a three-dimensional cracked body.

Figures 4-6 show the J-Q trajectories for all the studied geometry configurations. The J-Integral values were normalized by $J/b\sigma_0$, where b is the remaining ligament (W - a) and σ_0 is the yield strength of the material (400 MPa). To improve the visualization of the curves, the -Q values were represented in the x-axis.

The solid lines in Figs. 4-6 correspond to the results obtained for the plane-strain condition (denoted by PS). In this case, the J-Q trajectories were obtained considering a traditional 2-D Q evaluation, which takes into account only the in-plane constraint effect: the smaller the crack depth the larger the loss of constraint. Thus, the solid lines have the same aspects despite the specimen thickness variation from Fig. 4 to Fig. 6.

On the other hand, the marks in Figs. 4-6 represent the J-Q trajectories corrected with the proposed Q_{3D}-*Parameter*, which aims to capture both the in-plane and out-of-plane constraint effects. For all the studied specimens, the constraint effects are larger for the shallow cracks. It should be noticed that for crack sizes (denoted by the relationship a/W) inferior to 0.5, the values of (-Q) are negative, meaning that the specimen suffers a strong loss of constraint. Also, for smaller thickness the effects of the loss of constraint are larger. Such fact evidences

the strong removal of the plane-strain condition. Looking at Fig. 4-6, it can be observed that the J-Q trajectories corrected by Q_{3D}-*Parameter* are able to describe the global constraint level in an efficient way. This is evidenced by the coherence in the constraint level behavior with regard to the crack sizes and thickness of the specimens.

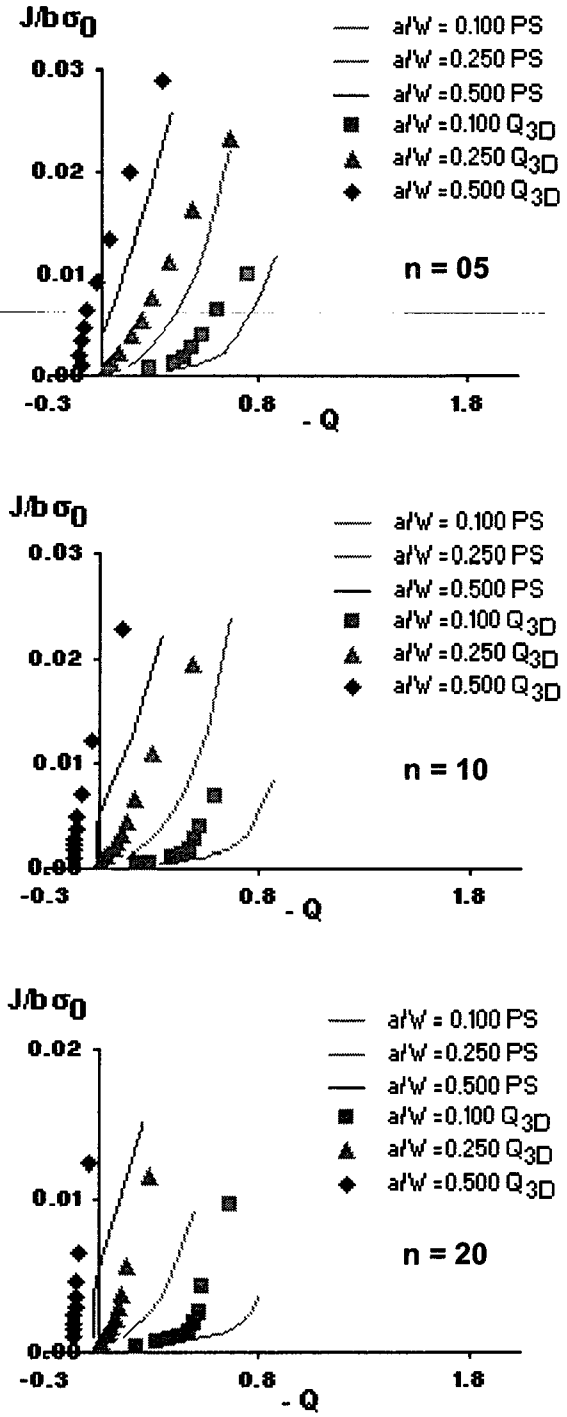

Figure 4- J-Q trajectories (Thickness ratio - B/W = 0.5)

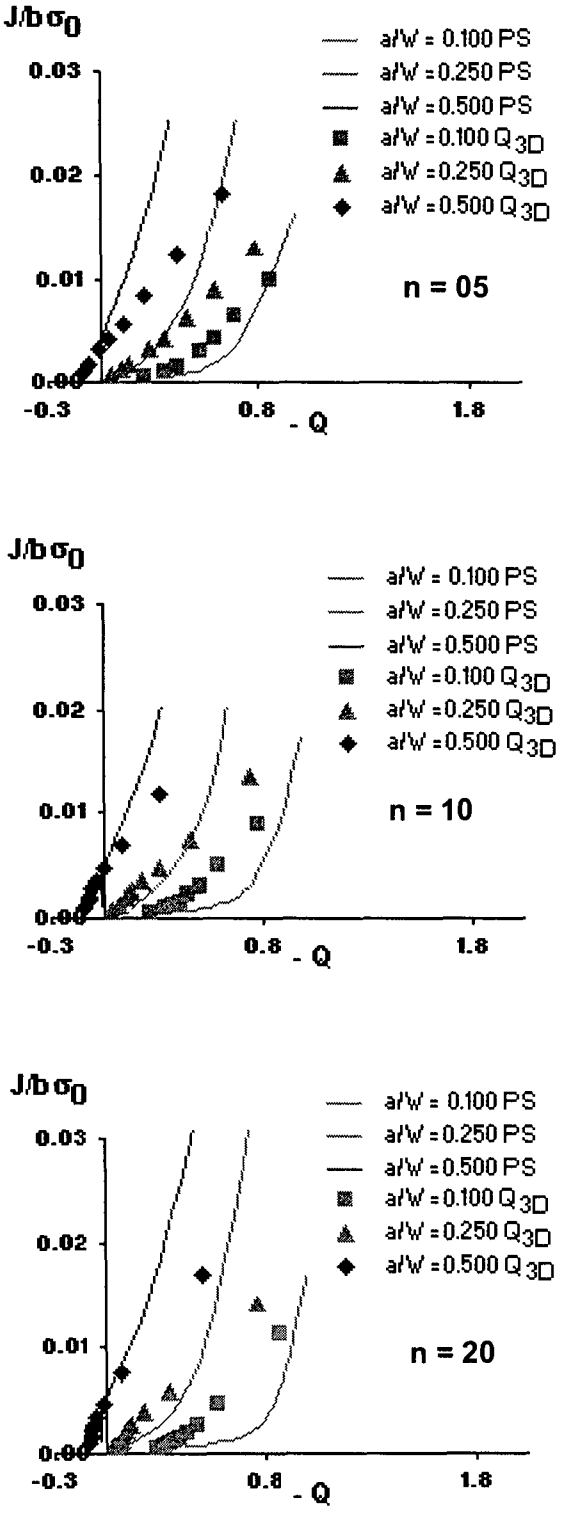

Figure 5- J-Q trajectories (Thickness ratio - B/W = 0.25)

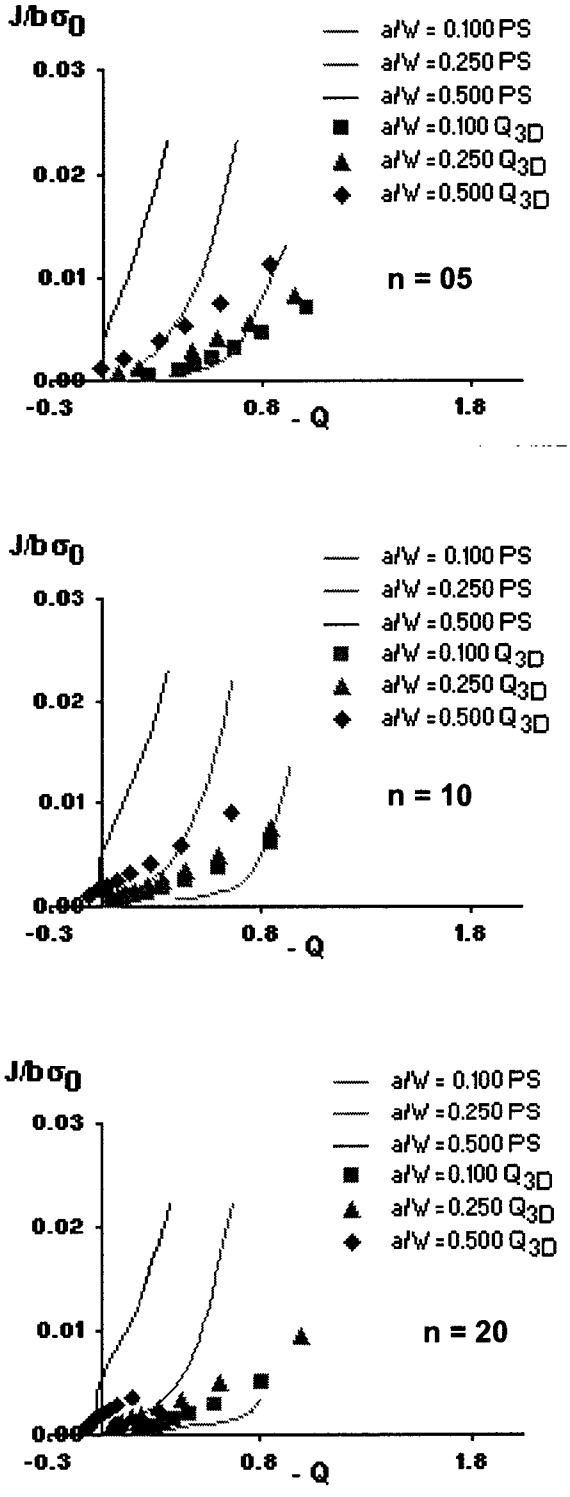

Figure 6- J-Q trajectories (Thickness ratio - B/W = 0.125)

5. CONCLUSIONS

This work presented the results of detailed three-dimensional finite element analyses carried out to study constraint effects in single-edge cracked bars in three point bend SE(B) specimens. Based on that systematic study, in which different relative crack lengths and thickness were considered, a new parameter was proposed to quantify crack tip constraint.

J-Q trajectories, corrected by the new parameter, were presented for all studied geometry configurations. The general behavior observed when the corrected trajectories were compared with the lines representing the plane-strain condition showed that a pattern can be established, so that the new parameter could be used as a viable alternative to quantify constraint effects.

Another important fact is the possibility of the use of the J-Q trajectories corrected by Q_{3D}-*Parameter* in support to micromechanical approaches for the study of ductile-fracture transition behavior of ferritic steels. It is known that in the master curve approach the influence of the specimen thickness is taken into account essentially by consideration of statistical effects. With a formulation based on the Q_{3D}-*Parameter*, the constraint effects due to specimen thickness could also be included.

Evidently, more investigation is necessary to make the new Q_{3D}-*Parameter* an effective parameter to be used in practical applications. This would include extensive finite element studies considering other specimen geometries as well as real tests in laboratory.

REFERENCES

Al-Ani, A.M., Hancock, J.W., 1991. J-dominance of short cracks in tension and bending. *Journal of Mechanics and Physics of Solids*, vol. 39, pp. 23-43

Cravero, S., Ruggieri, C., 2003. JQCRACK Versão 1.0 Cálculo numérico do parâmetro hidrostático Q para componentes estruturais 2D contendo trinca. *Boletim Técnico da Escola Politécnica da Universidade de São Paulo - BT/PNV/59*, Departamento de Engenharia Naval e Oceânica.

Huges, T.J., 1980. Generalization of selective integration procedures to anisotropic and nonlinear media. *International Journal for Numerical Methods in Engineering*, vol. 15, pp. 1413-1418.

Koppenhoefer, K., Gullerud, A., Roy, A., Walters, M., Dodds, R. H., 2002. WARP3D-Release 14.1: 3D Dynamic nonlinear fracture analysis of solids using parallel computers and workstations. *Structural Research Series 607*. UILU-ENG-95-2012, University of Illinois at Urbana-Champaign.

O'Dowd, N.P., Shih, C.F., 1991. Family of crack-tip fields characterized by triaxiality parameter: Part I – Structure of fields. *Journal of the Mechanics and Physics of Solids*, vol. 39, n. 8, pp. 989-1015.

O'Dowd, N.P., Shih, C.F., 1992. Family of crack-tip fields characterized by triaxiality parameter: Part II – Structure of fields. *Journal of the Mechanics and Physics of Solids*, vol. 40, pp. 939-963.

Shih, C.F., Moran, B., & Nakamura, T., 1986. Energy release rate along a three-dimensional crack front in a thermally stressed body. *International Journal of Fracture*, vol. 30, pp. 79-102.

Willians, M.L., 1957. *Journal of Applied Mechanics*, vol. 24, pp. 109-114.